SYNERGISTIC EFFECT OF POTASSIUM AND CALCIUM IONS ON COAL PYROLYSIS BEHAVIORS: EXPERIMENTAL AND KINETIC MODEL INVESTIGATIONS

Zhanwei LIANG[1]*, Jiafei QIAO[1], Xin YANG[2], Hongwei CHEN[3], Zheng ZHANG[2]

[1] CHN Energy New Energy Technology Research Institute Co., Ltd., Beijing City, China

[2]School of Water Conservancy and Electric Power, Hebei University of Engineering, Handan City, Hebei, China

[3]Key Laboratory of Condition Monitoring and Control for Power Plant Equipment, Ministry of Education, North China Electric Power University, Baoding City, Hebei Province, China

[*] Corresponding author; E-mail: liangzhanwei11@163.com

A low rank coal was first used to investigate the synergistic effect of inherent and loaded potassium and calcium ions on the pyrolysis behaviors. The non-isothermal thermal analysis with higher heating rate to medium pyrolysis temperature was carried out by thermogravimetric analyzer (TGA) for the selected raw and treated coal samples. Preliminary experiments conducted show that the particle size smaller than 160 μm can eliminate heat and mass transfer effect, and the most of volatile matter was released by heating the raw coal (R-coal) to 750 °C. Moreover, the effect of heating rate, inherent and loaded potassium and calcium on moisture evaporation and devolatilization is systematically investigated, and the devolatilization index (D) is introduced to estimate the activity of pyrolysis process. A comparison among the acid pickling coal (H-coal), acid pickling coal loaded with calcium (H-coal-C) and potassium (H-coal-P) shows that potassium and calcium have improved the inner water holding capacity. Finally, the influence of inherent and loaded potassium and calcium on the kinetic characteristics of volatile matter release stage was studied with Coats-Redfern integral method.

Key words*: low rank coal, potassium, calcium, pyrolysis behaviors, pyrolysis kinetic*

1. Introduction

Low rank coals are paid more attention for its distribution in several regions throughout the world, but its less conversion efficiency due to their high water, high oxygen functional group content, and low calorific value [1–3]. Thus, there were numerous studies on the treatment to upgrade low rank coal for improving char yields and properties [4–10]. The pyrolysis has been considered as the initial step in the utilization process of coal [11,12], which is a conversion process that allows the transformation of coal into gas, liquid and solid products [13]. Good understanding the mechanism of low rank coal pyrolysis will be beneficial to control the release of pollutants and enhance the conversion rate. Moreover, pyrolysis influences significantly the thermochemical conversion process

of gasification and liquefaction and also controls the combustion characteristics of coal ignition and flame stability [14–16].

A coal with potassium and calcium ions is a type of coal that is enriched with potassium and calcium ions in ash composition compared to other types of coals. The potassium and calcium ions in coal modified the structure through changing the interconnection between the macro molecules, thus affecting the pyrolysis properties and behavior of the coal, such as calorific value, volatile matter content, char reactivity and ratio of oil to tar [17–22]. Solomon *et al*. [17] demonstrated the role of exchangeable cations in cross-linking reactions by demineralizing these ions from Zap North Dakota lignite and introducing calcium cations in the oxidized Pittsburgh Seam bituminous coal. They found that demineralized lignite shows a lower rate of cross-linking due to the reduced mineral content. Wornat *et al*. [18] and Shibaoka *et al*. [19] revealed several effects of ion-exchanged calcium on the product tars for Yallourn brown coal, such as calcium causes a reduction in tar yield at pyrolysis temperature of 600–800°C by hindering the escape of large tar molecules or enhancing the opportunity for their conversion to char. Sathe *et al*. [20] and Li *et al*. [21] reported the hindering effect of Alkali and Alkaline Earth Metallic (AAEM) on the release of the larger aromatic ring systems, which decrease the yield of large molecules contained in the tar. Wu *et al*. [22] investigated the influences of volatile-char interactions on the volatilization of AAEM species for Victorian brown coal at pyrolysis temperature of 900°C.

To assess the applicability and optimize the pyrolysis process of coal, it is important to understand the thermal decomposition. Thermogravimetric analysis, as the most general method, is used to conduct thermal decomposition and perform kinetic studies [11, 13]. To predict the pyrolysis behavior of coal, many researchers focused on thermal decomposition kinetics of coal with the purpose of obtaining kinetic parameters.[11, 13, 23,24]. The Coats-Redfern method, based on the Coats and Redfern equation, is widely applied to estimate activation energy, pre-exponential and reaction order [13, 25]. Niu *et al*. [26] and Fei *et al*.[27] studied the kinetic characteristics of pyrolysis stages for three typical functional groups, including aliphatic groups, C–O and hydroxyl, by applying Coats-Redfern approximation. Their results show that the different pyrolysis stages of functional groups were fitted well with different kinetic models. Montiano *et al*. [13] and Kantarelis *et al*. [25] obtained the activation energies of coal and E-waste and introduced in the Coats-Redfern model to calculate the pre-exponential factors and reaction order. Therefore, Coats-Redfern method is one of most common and widely accepted and reliable methods in scientific community to estimate thermo-kinetic parameters from experimental data.

It can be concluded that the effect of single potassium or calcium on coal pyrolysis was studied in previous researches. According to the author's best knowledge, there was no study focusing on synergistic effects of inherent and loaded potassium and calcium on pyrolysis behaviors of a low rank coal, especially in the condition of higher heating rate to the medium pyrolysis temperature (750°C). Therefore, the aims of the present work is first to experimental investigate the synergistic effects of inherent and loaded potassium and calcium on the thermal decomposition stages of moisture evaporation and devolatilization, and the devolatilization index is introduced to estimate the reactivity of pyrolysis process. Moreover, kinetic parameters are calculated for the pyrolysis of raw coal and modified coal samples under N_2 using the Coats-Redfern method.

2. Experimental and modeling

2.1. Materials

A low rank coal, which comes from Zhundong coalfield of China, was collected as objective for the experiments. The proximate and ultimate analysis results of selected raw coal are shown in Table 1. The ash compositions of the raw coal are shown in Table 2. The coal is hard coal according the volatile matter. The analytical grade reagent of powdery K_2CO_3 (≥ 99% pure) and $Ca(OH)_2$ (≥ 95% pure), Nitric acid and hydrochloric acid solution were bought from Kermel Chemical Regent Tianjin Co. Ltd. and used as received. Nitrogen with purity higher than 99.99% was used to maintain an inert atmosphere at flow rate of 100 ml/min, which was supplied by North China Special Gas.

Table 1. The proximate and ultimate analysis of the raw coal

Proximate analysis (wt. %)				Ultimate analysis (wt. %)					Qar,L
Mar	FCar	Var	Aar	Car	Har	Nar	Oar	Sar	kJ/kg
30.7	41.62	24.63	3.05	53.84	2.68	0.50	8.86	0.37	19150

ar: As received basis; L: Low heating value.

Table 2. The ash compositions of the raw coal (wt. %)

SiO_2	Al_2O_3	Fe_2O_3	CaO	MgO	TiO_2	SO_3	K_2O	Na_2O	P_2O_5
14.48	8.11	3.90	39.67	6.92	0.73	18.82	0.67	5.42	0.21

2.2. Methods

The pyrolysis experiments were carried out in a TA instruments SDT Q600 thermoanalyser. Prior to heating, high purity N_2 was conducted into the inlet for 30 min to purge the air in the thermoanalyser. The sample weight of 10 mg (±0.05 mg) was heated from ambient temperature to 750°C under an Nitrogen flow rate of 100 ml min^{-1} at 20, 40, 60°C min^{-1}, respectively. Once the pyrolysis temperature reaches the preset final temperature, the experimental is shut off immediately, that is, there is no holding time for further heating.

The derivative of the weight loss curve was illustrated by obtaining the data of thermogravimetric analysis. In order to ensure the repeatability of the results, the tests were conducted at least two times, and the results were averaged from at least two times experiment data's.

The coal sample was partially dried at 105°C for more than 6 h. After cooling down, the coal was taken out, and then pulverized and sieved to obtain a powder of smaller than 160 μm in the particle diameter and stored in sealed bottles which were capped to isolate the sample from air. For brevity, the coal sample prepared without any treating is named the raw coal (R-coal). The raw coal was pickled in Nitric acid and Hydrochloric acid solution, respectively, to obtain acid pickling coal (H-coal). The detailed information of the acid pickling coal preparation can be found elsewhere [28]. The ash composition content of CaO, Na_2O and MgO for acid pickling coal dramatically decreases, however, the amount of K_2O increases slightly after acid pickling because the amount of K_2O in raw coal is too little to conducting further ion-exchange [28].

In preparation of the coal samples loaded with potassium and calcium, the impregnation method was used. Specific quantities of the additives were dissolved in a glass beaker using 100 ml deionized water. Then, the coal sample was immersed in the prepared additive solution and stirred 40 min with stirred rate of 800 r/min. The resulting mixtures were dried at 105°C for 12 h to constant mass and

stored in air-tight receptacles to prevent further changes. The R-coal impregnated with potassium and calcium is named the R-coal-P and R-coal-C, respectively. Similarly, the H-coal loaded with potassium and calcium is briefly expressed as H-coal-P and H-coal-C, respectively. The loading is referred to as the weight percent of additional in the total amount of the mixture. The K_2CO_3 and $Ca(OH)_2$ loading is 5 wt% and 3.2 wt%, respectively. This is a better selected loading amount, because it has higher effect on coal pyrolysis which has been conformed in our other experiments.

2.3. Kinetic modeling

Pyrolysis kinetic parameters were determined by applying the Coats-Redfern model, which derives from the Arrhenius equation and is an effective method for calculating the activation energy (*E*a) and pre-exponential factor (*A*) [25].

The general kinetic model that describes the conversion rate during pyrolysis under non-isothermal condition is usually described as the following Eq. (1):

$$\frac{dX}{dt} = k(T) \cdot f(X) \tag{1}$$

where $f(X)$ is a function that represents the reaction mechanism model and depends on the actual reaction mechanism, t is time, X is the conversion and $k(T)$ is the reaction constant that depends on the temperature.

The conversion in a pyrolysis process can be defined as:

$$X = \frac{m_0 - m_t}{m_0 - m_f} \tag{2}$$

where m_0, m_t and m_f represent the initial, actual and final weight percent of coal samples, respectively.

The temperature-dependent rate constant can be expressed by the Arrhenius equation as:

$$k(T) = A \cdot e^{-\frac{Ea}{RT}} \tag{3}$$

where A and Ea represent the pre-exponential factor and activation energy, respectively. R is the universal gas constant, and T is the Kelvin temperature. Considering the heating rate (h) is constant:

$$h = \frac{dT}{dt} = \frac{dT}{dX} \cdot \frac{dX}{dt} \tag{4}$$

The Eq. (4) can be written as:

$$\frac{dX}{dt} = h \cdot \frac{dX}{dT} \tag{5}$$

The fundamental model function $f(X)$ in Eq. (1) was summarized by White *et al*. [23] who listed the most common reaction mechanisms in solid state reactions. For chemical control and the reaction order N, $f(X)$ can take the form:

$$f(X) = (1 - X)^N \tag{6}$$

Introducing Eqs. (3), (5) and (6) into Eq. (1) the following expression is obtained:

$$\frac{dX}{(1-X)^N} = \frac{A}{h} \cdot e^{-\frac{Ea}{RT}} dT \tag{7}$$

Integrating Eq. (7) and applying the approximation of Taylor and assuming that $2RT/E$ is far less than 1, Eq. (8) are obtained [13]:

$$\ln\left[\frac{G(X)}{T^2}\right]=\ln\left(\frac{AR}{hEa}\right)-\frac{Ea}{RT}\quad\begin{cases}G(X)=-\ln(1-X) & N=1\\ G(X)=\dfrac{(1-X)^{1-N}-1}{(1-N)} & N\neq 1\end{cases} \tag{8}$$

3. Results and discussion

3.1. Effect of particle size and temperature on pyrolysis behaviors

Figure 1 presents the influence of particle size on the pyrolysis behavior of R-coal from ambient temperature to final temperature of 750°C. The extremely similar results of TGA and DTA curves for particle size of 80, 120 and 160 μm indicate that the size smaller than 160 μm can eliminate heat and mass transfer effect, even if at as high as heating rate of 40°C/min. The influence of temperatures on pyrolysis behavior of raw coal was shown in Fig. 2. It is can be seen that the pyrolysis curves of TGA and DTA at 850 and 900°C are almost same as the curve at 750°C. The weight loss is 35.7% before 750°C, and further enhancing the pyrolysis temperature to 850 or 900°C the weight loss increase 1.97 and 3.6%, respectively. It is concluded that the main weight loss occurs before 750°C, and there is only a small weight loss for further heating the raw coal to 850 or 900°C. Thus, it is enough to release most of the volatile matter by heating the raw coal to 750°C.

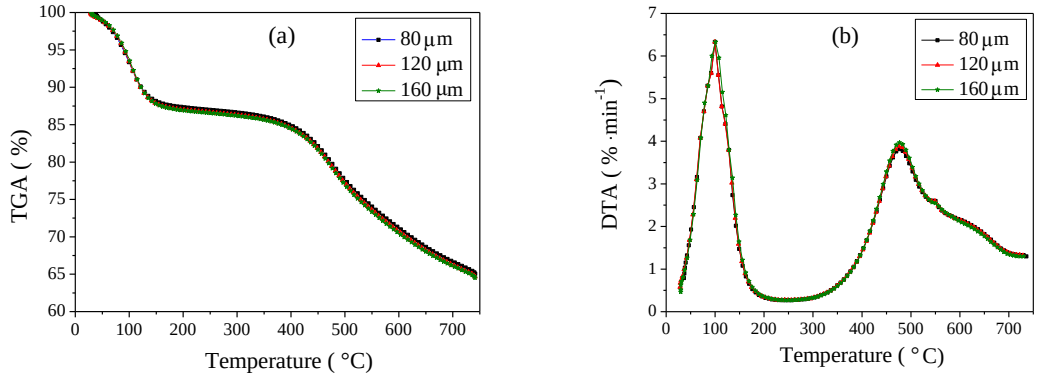

(a) TGA **(b) DTA**

Fig. 1. The influence of particle size on the pyrolysis behavior of R-coal with *h*=40°C/min

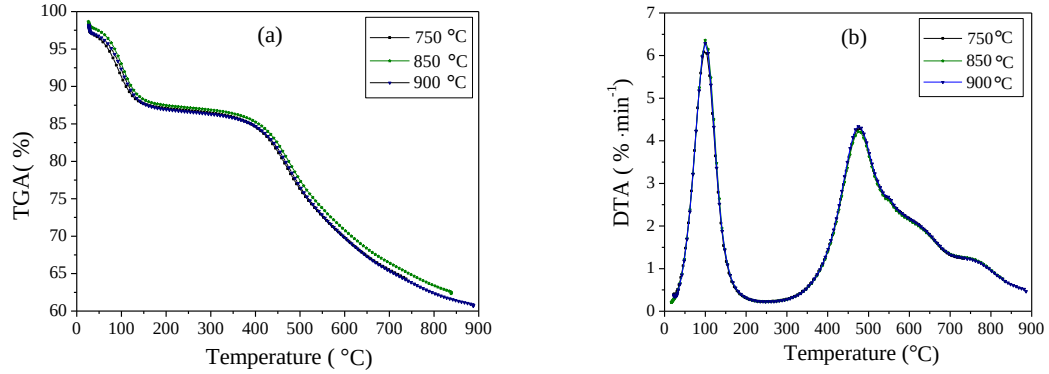

(a) TGA **(b) DTA**

Fig. 2. The influence of temperature on the pyrolysis behavior of R-coal with h=40°C/min

3.2. Effect of heating rate on pyrolysis behaviors

The pyrolysis temperature of raw coal increased from ambient temperature to 750°C at heating rates of 20, 40 and 60°C/min, respectively. The variations of TGA and DTA vs. temperature are shown in Fig. 3. The raw coal present two main decomposition stages, and the temperature of the maximum rate is between 86 and 111°C for the dewatering stage and between 462 and 480°C for devolatilization stage depending on the heating rate used. The peaks of DTA curves in Fig. 3(b) gradually become more intensive and move towards higher temperature with increasing the heating rate for both dewatering and devolatilization stages. This trend attributes to the raw coal reaches the required temperature in shorter times at higher heating rate, it is mean that the certain amounts of water or volatile matter must be released in shorter times. Thus the mass loss rate is higher with the increase of heating rate. Moreover, at lower heating rates the heating of the particles occurs more gradually with a more effective heat transfer to the inner parts of the particles, resulting in the water and volatile matter duly released from the particles. However, this action is delayed to higher temperature with increasing the heating rate and this trend is agreement with the previous results [13, 29,30].

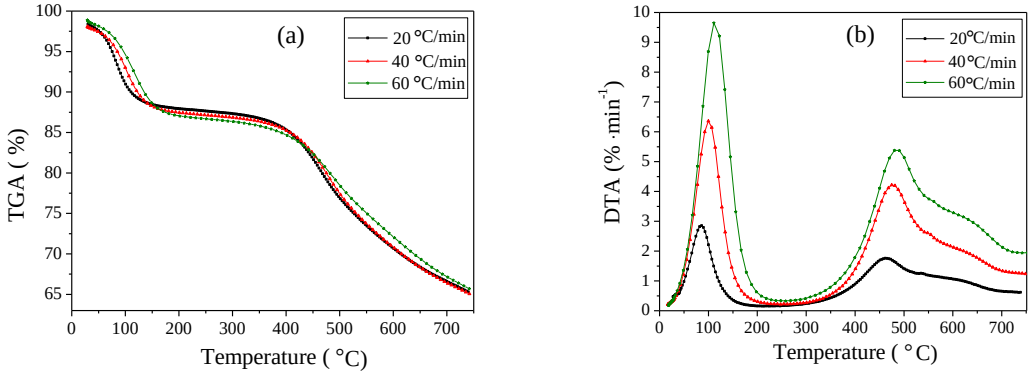

(a) TGA curves **(b) DTA curves**

Fig. 3. The influence of heating rate on the pyrolysis behavior

The devolatilization index (D) was defined to evaluate the volatile release property [28]:

$$D = R_{\max} \cdot R_{mean} / (t_{in} \cdot t_{\max} \cdot \Delta t_{1/2}) \quad (9)$$

where $R_{\max}$ and R_{mean} is the maximum and mean weight loss rate of volatile matter, respectively, $R_{\max} = (\mathrm{d}m/\mathrm{d}t)_{\max}$, $R_{\text{mean}} = (\mathrm{d}m/\mathrm{d}t)_{\text{mean}}$; t_{in} is the initial pyrolysis temperature, which corresponds to the minimum rate of volatile release at the end stage of drying and degassing water; $t_{\max}$ is the maximum weight loss temperature; $\Delta t_{1/2}$ is the temperature range when the value of $R/R_{\max}$ is 1/2; t_{f} is the final temperature of main pyrolysis process, $t_{\text{f}} = 2t_{\max}\text{-}t_{\text{in}}$. Pyrolytic parameters of R-coal with heating rate (R_{h}) of 20, 40, 60°C/min, respectively, are listed in Table 3.

The devolatilization index is applied to describe the volatile release property. As D described in Eq. (9) suggests that the larger of the value corresponds to higher release of volatile matter. The values of raw coal D at three heating rate are illustrated in Table 3. It is can be seen that the D increase with the heating rate, which is mean that the activity of pyrolysis is enhanced when raise the heating rate. This trend is agreement with the previous study [28].

Other pyrolytic parameters in Table 3 present that the t_{in}, $t_{\max}$, and t_{f} rise to high temperature with the increase of the heating rate, but the $\Delta t_{1/2}$ becomes narrower gradually. The values of $R_{\max}$

monotonically increase with increasing heating rate. The resulting pyrolytic parameters of raw coal for the three different heating rates in Table 3 are good agreement with the trend illustrated in Fig. 3.

3.3. Effect of potassium and calcium on pyrolytic behaviors

From Fig. 4(b) it can be seen that the R-coal DTA curves exhibit two main peaks, and the first peak is more intensive than that of second. The first peak corresponds to the maximum dehydration rate at 100°C and the second peak is the maximum weight loss rate of volatile matter which corresponds to the devolatilization temperature of 477°C. The dehydration peak is sharper than that of devolatilization, which demonstrates that the R-coal has high water content and it is confirmed by the proximate analysis in Table 1 and the weight loss of water in Table 4. The first peak is attributed to the most loss of water in voids and pores of coal [26]. The dehydration process is accompanied with desorption of N_2, CO_2 and CH_4 molecules before the end of dehydration temperature at 237°C [28].

In the devolatilization stage of R-coal after 237°C, some weak non-covalent bonds are initially cracked and the weak bonded compounds are slightly vaporized and gradually released from solid coal. Aliphatic group or oxygen-containing groups cracked slowly before 400°C attributed to the emission of small molecules embedded in the macro and micro pores or bonded by some weak non-covalent bond, such as hydrogen bonds or other even weaker interactions [26]. The OH bond content decrease through the following reactions at 130–460°C [26, 31]:

$$\text{Ph–OH} + \text{Ph}'\text{–OH} \rightarrow \text{Ph–O–Ph}' + H_2O \quad (10)$$

$$\text{Ph–OH} + \text{Ph}'\text{–}CH_3 \rightarrow \text{Ph–}CH_2\text{–Ph}' + H_2O \quad (11)$$

The maximum mass loss rate is conducted at 477°C by rising temperature because of the cleaving of bridge bonds, which produced free radical groups and subsequent production of gas and tar. The four C═O groups, such as ester, hydrogen bonded carbonyl or carboxyl, ketone (especially aromatic ketone) and quinone, start to decompose rapidly at approximately 370°C, and the cracking of aromatic C═C bonds and C–C bonds involved to strongly decomposition of aliphatic groups from approximately 400°C [26, 31]. The solid residue conducts further condensation reactions, which mainly releases two gases, such as CO and H_2.

The shape of TGA and DTA curves illustrated in Fig. 4 are similar between the R-coal and H-coals. It is concluded that the main structure in the raw coal does not change after acid pickling. However, the water content in H-coal is dramatically lower than that of R-coal, which is quantitatively presented in Table 4. In comparison, H-coal initial devolatilization takes place at lower temperature, but its weight loss rate of volatile matter is entirely higher after 200°C. While there is more volatile matter conducted from H-coal as shown in Table 4. The DTA curves for both R-coal and H-coal in Fig. 4(b) exhibit the maximum weight loss rates in dewatering and devolatilization stage corresponding to almost the same temperature at 100 and 470°C, respectively.

A comparison of pyrolytic parameters between R-coal and H-coal in Table 3 shows that the index *D* of H-coal is larger than that of R-coal, which means that the H-coal is more activity than R-coal in devolatilization stage. The other parameters shown in Table 3 are accord with the trend presented in Fig. 4.

The R-coal was dried at 105°C before conducting pyrolysis experimental which caused much of water loss. Thus the water content contained in raw coal (30.7% in Table 1) is much higher than that in dried raw coal (13.69% in Table 4). However, the water content of H-coal is only 3.51%, indicating acid pickling procedure removing most of water due to the ion-exchange and hydrothermal treatment.

Therefore, the different in dehydrating property for R-coal and H-coal partially attributes to the effect of inherent potassium and calcium on the water holding capacity. It can be seen that the inherent potassium and calcium contained in raw coal can improve the water holding capacity. Moreover, the decrease of water holding capacity may due to the acid pickling procedure. The hydrothermal treatment was used in the process of acid pickling of coal samples, which was considered as an effective pretreatment method to reduce water in coals [5, 26]. The water soluble in-organics and hydrophilic organics containing oxygen functional groups may be dissolved and leached out with the water during hydrothermal treatment [9, 32].

In addition, the second peak value of R-coal is 3.9%·min^{-1} at temperature of 477°C, which is lower than that of H-coal of 4.3%·min^{-1} at temperature of 473°C. The R-coal pyrolysis required more energy to break the molecular units in the coal network than that of H-coal. The high energy consumption during devolatilization is dependent on the effect of inherent potassium and calcium in a great extent; especially the metal ion can be available to ion-exchange. The ion-exchange potassium and calcium can perform interconnection function in the coal fragment structure which increases the energy of molecule escaping from the coal. This connect function reduced the ratio of tar production when studied the brown coal pyrolysis [18,19].

The *D* values of R-coal and H-coal are 5.99 and 39.6, respectively, and the *D* of H-coal is approximately 7 times larger than that of R-coal. It can be concluded that the inherent potassium and calcium, especially the calcium ion which presents the largest ion-exchange before and after acid pickling [28].

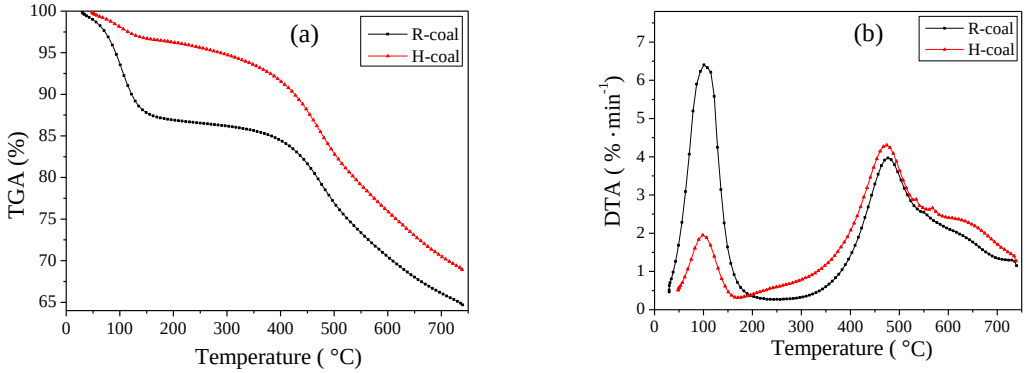

(a) TGA curves and (b) DTA curves

Fig. 4. Effect of inherent potassium and calcium on pyrolysis behavior of R-coal and H-coal with *h*=40°C/min

A thermal decomposition is utilized to evaluate the effects of loaded potassium and calcium on the R-coal pyrolysis behavior. Figure 5 illustrated the thermal characteristics of R-coal loaded with K_2CO_3 and $Ca(OH)_2$. The shape of TGA and DTA curves illustrated in Fig. 5 are similar for the R-coal, R-coal-P (loaded with 5% K_2CO_3) and R-coal-C (loaded with 3.2% $Ca(OH)_2$), which indicates that the main structure in the raw coal does not influence by loading potassium and calcium.

The DTA curves exhibit two main peaks in Fig. 5(b). The first peak intensities are 6.36, 2.75 and 4.13 %/min^{-1} at 99.6, 102.9 and 99°C for R-coal, R-coal-P and R-coal-C, respectively. From Fig. 5 it can be seen that the water of R-coal-P and R-coal-C is lower than that of R-coal, which indicates the raw coal loaded with potassium and calcium presenting lower water holding capacity. This trend shows a reverse way when compared with the improving effect of potassium and calcium on water holding capacity. This phenomenon mainly ascribes to the hydrothermal treatment, which was used in

the process of potassium and calcium loading. The inherent and loaded potassium and calcium in R-coal-P and R-coal-C can improve the water holding capacity to a certain extent, but the hydrothermal treatment largely reduces its capacity and the effect of potassium and calcium on the capacity is much lower by comparison with hydrothermal treatment.

The devolatilization peak intensities are 3.97, 3.64 and 3.65 %/min^{-1} at 477, 473.2 and 480.2°C for R-coal, R-coal-P and R-coal-C, respectively. The final mass of the R-coal loaded with K_2CO_3 and $Ca(OH)_2$ is higher than R-coal under the same pyrolysis condition, which is mainly due to the influence of water in coal samples. In detail, it can be seen that the water of R-coal shown in Table 4 (13.69%) is higher than that of R-coal-P and R-coal-C, which is attribute to the hydrothermal treatment on the R-coal-P and R-coal-C resulting in lower water holding capacity. It also shows that the amount of volatile matter is highly dependent on the water in coal samples as presented in Table 4.

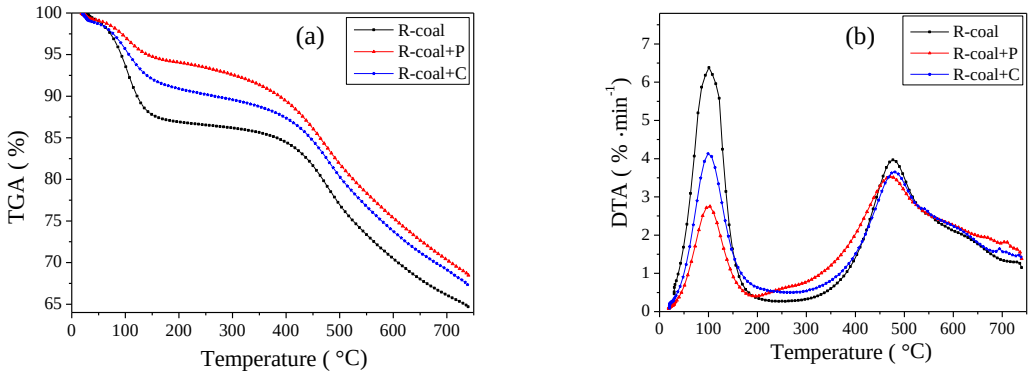

(a) TGA curves **(b) DTA curves**

Fig. 5. Effect of loaded potassium and calcium on pyrolysis behavior of R-coal with *h*=40°C/min

The values of *D* (in Table 3) are 26.35, 21.89 and 22.73 for R-coal, R-coal-P and R-coal-C, respectively. This result implies that the raw coal loaded with potassium and calcium shows lower activity than that of raw coal alone and K_2CO_3 has a higher inhibitory action on the pyrolysis of R-coal than that of $Ca(OH)_2$.

To further confirm the effect of potassium and calcium on the pyrolysis behavior, the following experimental was conducted as illustrating in Fig. 6. Specifically, all the samples are firstly treated with acid pickling which contains the hydrothermal treatment procedure, and then the K_2CO_3 and $Ca(OH)_2$ were impregnated on the H-coal. From the shape of curves, it is also concluded that the main structure in the raw coal does not change after treating by above methods.

The results shown in both Fig. 6 and Table 4 clearly indicate that the potassium and calcium have improved the water holding capacity, and the H-coal-C contains higher water content than H-coal-P. Moreover, the amount of volatile matter increases with decreasing the water content. The value of *D* for H-coal-P and H-coal-C is lower than H-coal which indicates that the potassium and calcium can partially inhibit the activity of coal pyrolysis.

However, the experimental result shows that the weight loss rate of H-coal-P-C is higher than that of H-coal when simultaneously loading K_2CO_3 and $Ca(OH)_2$ on the H-coal. While the value of D for H-coal-P-C is much higher than that of H-coal, indicating the H-coal-P-C presenting higher activity than H-coal.

The initial temperatures (t_{in}) listed in Table 3 vary in different coal samples. When making a comparison of these samples, it can be found that R-coal, R-coal-C and H-coal-C have higher initial

temperature. Thus, it is supposed that initial temperature increase if the coal samples contain calcium. However, it has lower initial temperature that the samples contain both calcium and potassium ions, such as R-coal-P and H-coal-P-C, which possibly resulting in the potassium offsetting calcium action. A comparison of H-coal and H-coal-P shows that the sample contains potassium has higher initial temperature, since potassium contained sample improves the initial temperature. Summarily, the potassium and calcium can improve the initial temperature, and the effect of potassium is strongly lower than calcium, but the potassium can offset the effect of calcium on initial temperature improving.

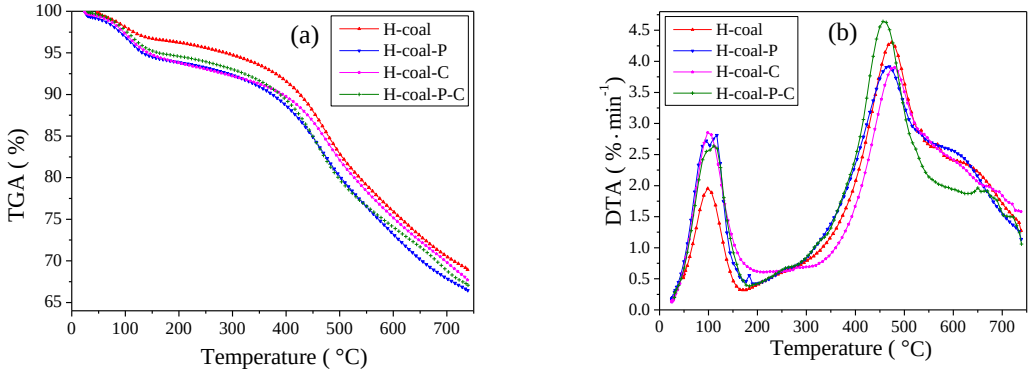

(a) TGA curves **(b) DTA curves.**

Fig. 6. Effect of loaded potassium and calcium on pyrolysis behavior of H-coal and with *h*=40°C/min

Table 3. Pyrolytic parameters of coal samples

samples	R_h (°C/min)	t_{in} (°C)	t_{max} (°C)	$(dw/dt)_{max}$ (%·min^{-1})	t_f (°C)	$\Delta t_{1/2}$ (°C)	D (10^{-8}·%^{2}·°C^{-3}·min^{-2})
R-coal	20	219.1	461.4	1.7587	703.7	245.3	5.99
	40	237.1	477.3	3.9674	717.5	241.2	26.35
	60	258.3	485.3	5.4065	712.3	237.1	44.51
R-coal-P	40	195.3	473.2	3.5362	751.1	326.3	21.89
R-coal-C	40	258	480.2	3.6541	702.4	244	22.73
H-coal	40	172.8	474.3	4.3065	775.8	255.3	39.60
H-coal-P	40	196.4	466.6	3.9237	736.8	280.6	30.56
H-coal-C	40	231	477.9	4.0923	724.8	234.2	30.69
H-coal-P-C	40	183.3	458.8	4.6507	734.3	140	77.93

Table 4. The weight loss of water and volatile matter of coal samples

	R-coal	R-coal-P	R-coal-C	H-coal	H-coal-P	H-coal-C	H-coal-P-C
m_W	13.69	5.88	9.91	3.51	6.09	6.67	5.23
m_V	21.61	25.62	22.73	27.52	27.46	25.59	27.69

m_W: the weight loss of water content, %; m_V: the weight loss of volatile matter, %.

3.4. Kinetic model

Coal pyrolysis kinetic is a considerably complex process, and was investigated by many studies with thermogravimetric analysis by using the percent of mass loss as the conversion rate [26, 33–36]. However, there were few reports on kinetic analysis of low rank coal based on the heating rate of 40 °C/min to pyrolysis temperature of 750 °C. In this study, we intend to study the influence of

inherent and loaded potassium and calcium on coal samples pyrolysis kinetic characteristics with the heating rate of 40°C/min to medium pyrolysis temperature of 750°C. Preliminary experiments carried out in section 3.1 shown that there were no resistances, such as heat and mass transfer, might influence the thermogravimetric analysis and the results derived from the kinetic study.

The first-order reaction mechanism model was firstly taken to obtain the kinetic parameters. If there is small difference between the values of R^2 for different orders (N), the simplest one would be chosen. When the N is considered to be 1 for the present research work, all plots divided two stages in Fig. 7 show linear correlation coefficients bigger than 0.97, and thus as N=1 the Eq. (8) can be finely used to calculate the Ea and A. By plotting $\ln[G(X)/T^2]$ vs. $1/T$ for the two stages, it is possible to obtain E and A from the slope and intercept of the lines, respectively, which shown in Fig. 7. The results calculated from Fig. 7 are presented in Table 4.

The Ea values are many differences as the different coal and their heterogeneity, and the activity energy of coal is different due to the heterogeneity of the samples and the complex nature of the reactions [25]. A wide range of activation energy from 8.6 to 143.6 kJ/mol was obtained by Niu *et al.* [26] for a perhydrous bituminous coal using non-isothermal low temperature pyrolysis.

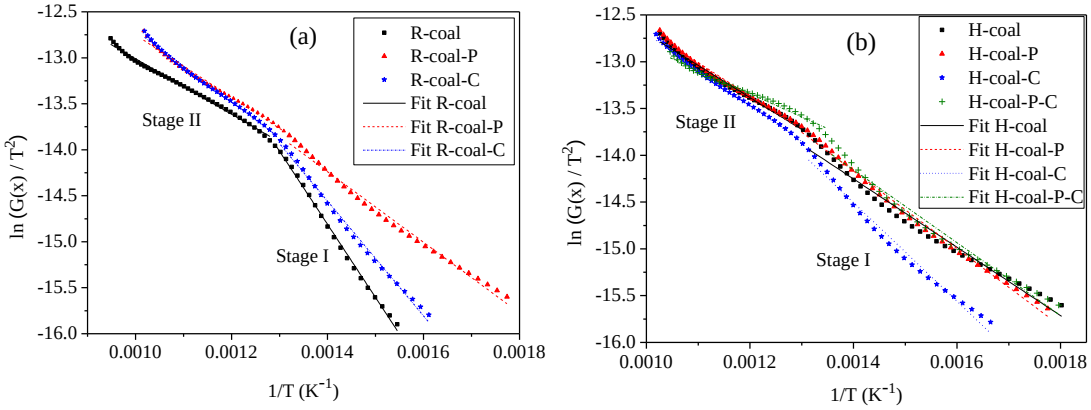

(a) R-coal and its mixtures **(b) H-coal and its mixtures**

Fig. 7. Plots for determination of *E* and *A* by Coats-Redfern method according to the first-order reaction model

From Table 5, it can be seen clearly that the values of Ea in stage I are bigger than that in stage II for each coal samples, which indicates that the activity of stage I is lower than stage II. This suggests that decomposition of stage I dominates the primary pyrolysis of coal samples. Moreover, a lower activity indicates that the volatile matter decomposes more slowly and that the reaction rate is slower than that of higher activity. The activation energy is ascribed from the various of decomposition mechanisms, which involve multiple processes during pyrolysis [13,25]. The activation energy of stage I is higher than stage II due to the different nature of the processes taking place between the two stages, which may have been related to the evaporation of highly volatile compounds present in coal in stage I and light volatile matter in stage II.

The value of Ea for R-coal in stage I is higher than that of R-coal-P and R-coal-C, however, it becomes the lowest one for the three samples in stage II. Thus it can be concluded that the potassium and calcium loaded in the raw coal improved the activity in stage I, especially the potassium, and exhibited inhibition in stage II. The inherent potassium and calcium present the same action as the loaded one based on detailed comparison between R-coal and H-coal in Table 5. While the Ea value of H-coal is smaller by comparison with H-coal-P and H-coal-C for both the two stage. This means that both calcium and potassium inhibit the activity of H-coal, especially for calcium. However, the H-

coal-P-C shows special trend in comparison with H-coal which is different from the above description. The *E*a of H-coal-P-C is slightly higher than H-coal in stage I, and then it strongly smaller in stage II, which shows that it is almost the most active sample presented in Table 5.

By using the activation energy and pre-exponential factor in Table 5 it is possible to calculate the conversion for all the samples. The simulation was carried out for a conversion interval between 0.05 and 0.95 and the results were presented in Fig. 8. The calculated conversions vs. kelvin temperature are in very good agreement with the experimental results except for H-coal that underestimate the experimental data at range of 740–767 K. This deviation is attributed to the fitting error of H-coal in stage I presented in Fig. 7 (b), and the R^2 value of H-coal is smaller than 0.98 shown in Table 5 also illustrated the deviation between the simulated and experimental conversion. In general the values of R^2 obtained between calculated and experimental conversions are higher than 0.98, although in the case of the H-coal in stage I, the correlation coefficient is slightly lower, it is enough high to be accepted.

Table 5. Kinetic parameters of coal samples using Coats-Redfern model

Samples	Stage I				Stage II			
	t_I (°C)	R^2	*E*a (kJ/mol)	*A* (min^{-1})	t_{II} (°C)	R^2	*E*a (kJ/mol)	*A* (min^{-1})
R-coal	273.1–508.1	0.9974	66.11	8040	508.1–750	0.9950	25.08	5.51
R-coal-P	195.3–490.2	0.9914	31.93	21.76	490.2–750	0.9891	28.20	11.68
R-coal-C	258–502	0.9950	51.87	737.63	502–750	0.9955	32.31	23.04
H-coal	172.8–496.1	0.9778	30.37	15.69	496.1–750	0.9880	28.45	12.83
H-coal-P	196.4–502	0.9937	34.45	38.53	502–750	0.9884	29.88	16.75
H-coal-C	231–496.1	0.9861	43.83	169.70	496.1–750	0.9956	31.93	21.82
H-coal-P-C	183.3–467.6	0.9829	32.37	25.82	467.6–750	0.9839	20.71	3.18

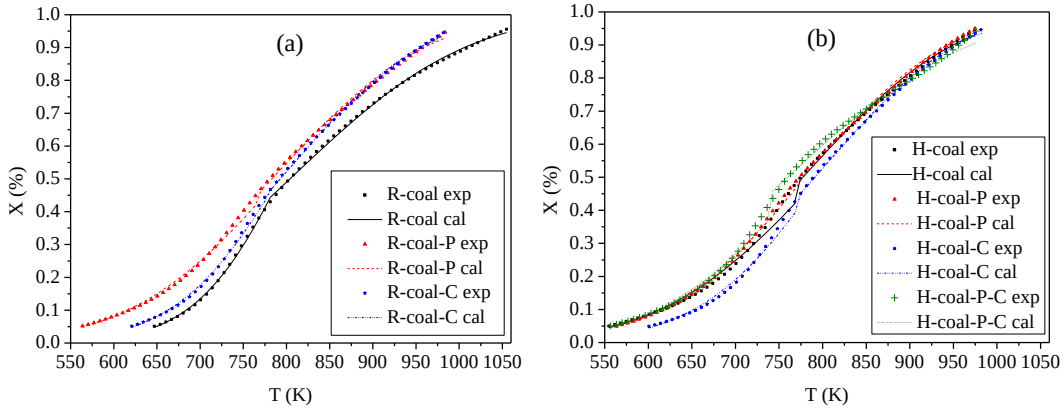

Fig. 8. Comparison between experimental and calculated results using Coats-Redfern model for coal samples

4. Conclusions

This study selected a low rank coal for the investigation of the non-isothermal pyrolysis behavior below 750°C in N_2 flow. The results indicate that the particle size smaller than 160 μm can eliminate heat and mass transfer effect, even if at as high as heating rate of 40°C/min, and it is enough to release most of the volatile matter by heating the raw coal to 750°C. The peaks of DTA curves gradually become more intensive and move towards higher temperature with increasing the heating

rate for both dewatering and devolatilization stages. The devolatilization index increase with the heating rate, which is mean that the activity is enhanced when raising the heating rate.

H-coal initial devolatilization takes place at lower temperature than R-coal, but its weight loss rate of volatile matter is entirely higher after 200°C, while there is more volatile matter conducted from H-coal. In addition, the second peak value of R-coal is 3.9%·min^{-1} at temperature of 477°C, which is lower than that of H-coal of 4.3%·min^{-1} at temperature of 473°C. The devolatilization index values of R-coal and H-coal are 5.99 and 39.6, respectively, and the devolatilization index of H-coal is approximately 7 times larger than that of R-coal. The inherent and loaded potassium and calcium in R-coal-P and R-coal-C can improve the water holding capacity to a certain extent, but the hydrothermal treatment largely reduces its capacity and the effect of potassium and calcium on the capacity is much lower by comparison with hydrothermal treatment. However, the results shown in both Fig. 6 and Table 4 clearly indicate that the potassium and calcium have improved the water holding capacity, and the H-coal-C contains higher water content than H-coal-P. The value of devolatilization index for H-coal-P and H-coal-C is lower than H-coal which indicates that the potassium and calcium can partially inhibit the activity of coal pyrolysis.

In this study, the Coats-Redfern model was used to study the influence of inherent and loaded potassium and calcium on coal samples pyrolysis kinetic characteristics. The value of *E*a for R-coal in stage I is higher than that of R-coal-P and R-coal-C, however, it becomes the lowest one for the three samples in stage II. While the *E*a value of H-coal is smaller by comparison with H-coal-P and H-coal-C for both the two stage. This means that both calcium and potassium inhibit the activity of H-coal, especially for calcium.

Acknowledgment

Research Foundation of Education Bureau of Hebei Province of China [ZD2020182]; Handan Science and Technology Project [19422121008-37].

References

[1] Katalanbula, H., Gupta, R., Low-grade coals: a review of some prospective upgrading technologies, *Energy Fuels*, *23* (2009), pp. 3392–3405

[2] Yang, X., *et al.*, Effects of K_2CO_3 and $Ca(OH)_2$ on CO_2 gasification of char with high alkali and alkaline earth metal content and study of different kinetic models, *Thermal Science, 26* (2022), 1, Part A, pp. 119–133

[3] Zhang, Z., *et al.*, Catalytic Effect of Inherently-Water-Soluble Sodium on Zhundong Coal Gasification, *Science of Advanced Materials*, *12* (2020), pp. 1019–1026

[4] Chen, Z., *et al.*, Steam-drying of coal. Part 1 Modeling the behavior of a single particle, *Fuel*, *79* (2000), pp. 961–973

[5] Favas, G., Jackson, W.R., Hydrothermal dewatering of lower rank coals 2 Effect of coal characteristics for a range of Australian and international coals, *Fuel*, *82* (2003), pp. 56–69

[6] Bergins, C., Kinetics and mechanism during mechanical/thermal dewatering of lignite, *Fuel, 82* (2003), pp. 355–364

[7] Zeng, C., *et al.*, Effects of thermal pretreatment in helium on the pyrolysis behaviour of Loy Yang brown coal, *Fuel*, *84* (2005), pp. 1586–1592

[8] Zeng, C., *et al.*, Effects of pretreatment in steam on the pyrolysis behavior of Loy Yang brown coal, *Energy Fuels*, *20* (2006), pp. 281–286

[9] Morimoto, M., *et al.*, Low rank coal upgrading in a flow of hot water, *Energy Fuels*, 23 (2009), pp. 4533–4539

[10] Shui, H., *et al.*, Hydrothermal treatment of a sub-bituminous coal and its use in coking blends, *Energy*

Fuels, *27* (2013), pp. 138–144
[11] Zellagui, S., *et al.*, Pyrolysis of coal and woody biomass under N_2 and CO_2 atmospheres using a drop tube furnace-experimental study and kinetic modeling, *Fuel Processing Technology*, *148* (2016), pp. 99–109
[12] Zhou, H., *et al.*, Oxygen release and attrition study of MgO supported Cu–Mn compounds as an oxygen carrier, *Science of Advanced Materials*, *12* (2020), pp. 1782–1789
[13] Montiano, M. G., *et al.*, Kinetics of co-pyrolysis of sawdust, coal and tar, *Bioresource Technology*, *205* (2016), pp. 222–229
[14] Solomon, P. R., *et al.*, Progress in coal pyrolysis, *Fuel*, *72* (1993), pp. 587–597
[15] Ofosu, A. K., *et al.*, Preparation and pyrolysis of O-(alkylphenyl) methyl and O-(alkylnaphthyl) methyl Illinois No. 6 coals. Role of dealkylation reaction in gaseous hydrocarbon formation, *Energy Fuels*, *2* (1988), pp. 511–522
[16] Monthìoux, M., Expected mechanisms in nature and in confined-system pyrolysis, *Fuel*, 67(1988), pp. 843–847
[17] Solomon, P. R., *et al.*, Cross-linking reactions during coal conversion, *Energy Fuels*, *4* (1990), pp. 42–54
[18] Wornat, M. J., Nelson, P. F., Effects of ion-exchanged calcium on brown coal tar composition as determined by fourier transform infrared spectroscopy, *Energy Fuels*, *6* (1992), pp. 136–142
[19] Shibaoka, M., *et al.*, Application of microscopy to the investigation of brown coal pyrolysis, *Fuel*, *74* (1995), pp. 1648–1653
[20] Sathe, C., *et al.*, Effects of heating rate and ion-exchangeable cations on the pyrolysis yields from a Victorian brown coal, *Energy Fuels*, *13* (1999), pp. 748–755
[21] Li, C. Z., *et al.*, Fates and roles of alkali and alkaline earth metals during the pyrolysis of a Victorian brown coal, *Fuel*, *79* (2000), pp. 427–438
[22] Wu, H., *et al.*, Volatilisation and catalytic effects of alkali and alkaline earth metallic species during the pyrolysis and gasification of Victorian brown coal, Part III The importance of the interactions between volatiles and char at high temperature, *Fuel*, *81* (2001), pp. 1033–1039
[23] White, J. E., *et al.*, Biomass pyrolysis kinetics: a comparative critical review with relevant agricultural residue case studies, *Journal Analytical and Applied Pyrolysis*, *91* (2011), pp. 1–33
[24] Wu, Z., *et al.*, Thermochemical behavior and char morphology analysis of blended bituminous coal and lignocellulosic biomass model compound co-pyrolysis: Effects of cellulose and carboxymethylcellulose sodium, *Fuel, 171* (2016), pp. 65–73
[25] Kantarelis, E., *et al.*, Thermochemical treatment of E-waste from small household appliances using highly pre-heated nitrogen-thermogravimetric investigation and pyrolysis kinetics, *Applied Energy*, *88* (2011), pp. 922–929
[26] Niu, Z., *et al.*, Investigation of mechanism and kinetics of non-isothermal low temperature pyrolysis of perhydrous bituminous coal by in-situ FTIR, *Fuel*, *172* (2016), pp. 1–10
[27] Fei, Y,. *et al.*, Comparison of some physico-chemical properties of Victorian lignite dewatered under non-evaporative conditions, *Fuel*, *84* (2006), pp. 1987–1991
[28] Qiu, P., *et al.*, Effects of alkali and alkaline earth metallic species on pyrolysis characteristics and kinetics of zhundong coal, *Journal of Fuel Chemistry and Technology*, *42* (2014), pp. 1178–1189
[29] Barriocanal, C., *et al.*, On the relationship between coal plasticity and thermogravimetric analysis, *Journal Analytical and Applied Pyrolysis*, *67* (2003), pp. 23–40
[30] Damartzis, T. H., *et al.*, Thermal degradation studies and kinetic modeling of cardoon (Cynara cardunculus) pyrolysis using thermogravimetric analysis (TGA), *Bioresource Technology*, *102* (2011), pp. 6230–6238
[31] Gavalas, G. R., *Coal pyrolysis*, Elsevier Scientific Publishing Company, New York, USA, 1982
[32] Svabova, M., *et al.*, Water vapour adsorption on coal, *Fuel*, *90* (2011), pp. 1892–1899
[33] Solomon, P. R., Hamblen, D. G., Finding order in coal pyrolysis kinetic, *Progress in Energy Combustion Science*, *9* (1983), pp. 323–361
[34] Solomon, P. R., *et al.*, Coal pyrolysis:experiments, kinetic rates and mechanisms, *Progress in Energy Combustion Science*, 1*8* (1992), pp. 133–220
[35] Khare, P., *et al.*, Application of chemometrics to study the kinetics of coal pyrolysis: a novel approach, *Fuel*, *90* (2011), pp. 3299–3305
[36] Wu, D., *et al.*, Investigation on structural and thermodynamic characteristics of perhydrous bituminous coal by Fourier transform infrared spectroscopy and thermogravimetry/mass spectrometry, *Energy Fuels*, *28* (2014), pp. 3024–3035

Submitted: 05.03.2022.
Revised: 14.05.2022
Accepted: 17.05.2022.